Hindawi
Advances in Materials Science and Engineering
Volume 2022, Article ID 8265019, 14 pages
https://doi.org/10.1155/2022/8265019

Research Article

Mechanical Behavior of High-Strength Bolted Joints Fabricated from Fire-Resistant Steel at Elevated Temperatures

Yuedong Wang,[1,2] **Xiaorun Li**,[3] **Peng Liu**,[4] **Changdong Wu**,[3] **Chuhan Liu**,[3] **Lijing Zeng**,[1] **Wentao He**,[3] **and Tiantian Yin**[3]

[1]*Central Research Institute of Building and Construction Co. Ltd, MCC Group, Beijing 100088, China*
[2]*Tsinghua University, Beijing 100084, China*
[3]*China Jingye Engineering Co. Ltd, Beijing 100088, China*
[4]*Yatai Construction Science & Technology Consulting Institute Co. Ltd., Beijing 100120, China*

Correspondence should be addressed to Xiaorun Li; lixiaorun2000@sina.com

Received 12 July 2022; Revised 12 October 2022; Accepted 26 October 2022; Published 15 November 2022

Academic Editor: Dora Foti

The use of fire-resistant steel is an effective way to alleviate fire safety issues in steel structures. Considering the limited research on bolted joints fabricated from fire-resistant steel, this study presents the results of the experimental investigation on the mechanical behavior of 40 specimens of bolted joints at room temperature and elevated temperatures (20°C~700°C). These specimens are assembled with fire-resistant steel plates and fire-resistant high-strength bolts (or ordinary high-strength bolts). The mechanical behavior of these specimens was investigated, which included the failure mode, deformation performance, and degradation of bearing capacity. The experimental results show that the treatment of the friction surface (specifically, impeller blasting and sprayed hard quartz sand) has a negligible effect on the ultimate strength of specimens and a relatively significant effect on the slip strength. In addition, reduction factors of the tensile strength (K_N) and slip strength (K_S) for both fire-resistant bolt specimens and ordinary high-strength bolt specimens decrease with the increase in temperature, especially in the case of elevated temperatures ranging from 400°C to 700°C. Prediction models with different reliability degrees are proposed to calculate the degradation of tensile strength under elevated temperatures, which has the potential to be used for the fire-resistant design of steel connections and structures.

1. Introduction

Steel has been used extensively in construction, followed by issues of fire resistance and elevated temperature resistance of steel structures [1]. In the case of fire, the mechanical properties of ordinary steel (such as strength and elastic modulus) will degrade sharply with the increase in temperature [2]. When the external temperature exceeds 600°C, ordinary steel will lose most of its strength and stiffness. For ordinary steel members without fire protection, the temperature can usually rise to more than 600°C within 20 minutes of the fire event. Therefore, scholars have carried out research and production of high-strength and fire-resistant steel, some of which have been applied in practical engineering.

As the main connecting means of a steel structure, high-strength bolts play an important role in the seismic properties of a steel structure. Elevated temperature results in additional stress caused by the thermal expansion of components [3], which reduces the bearing capacity of high-strength bolts and thus easily leads to connection failure. In steel structures, a premature connection failure has a negative impact on the overall performance of the structure and even brings about structural damage and collapse. Consequently, the mechanical properties of high-strength bolts at high temperatures have attracted academic attention. Lawson [4] conducted fire resistance experiments on beam-column joints with high-strength bolts and found that the temperature in the bolt is much lower than that in the bottom flange of the beam when the joint is damaged. Chen

and Wang [5] investigate how connection details affect structural survivability at high temperatures based on parametric simulations. Theodorou [6] obtained that the strength of high-strength grade 8.8 bolts began to decline rapidly after 300°C, and at 600°C, its ultimate strength had decreased to 35% of the ultimate strength under normal temperature. Król and Wachowski [7] found that the temperature level of the fire, fire duration, and fire-fighting method significantly affect the bolts' mechanical properties. Lange and González [8], Lou et al. [9], and Zhu et al. [10] studied the mechanical properties, slip coefficient, and pretension force of high-strength grade 10.9 bolts at high temperatures. Hanus et al. [11] investigated the mechanical behavior of high-strength grade 8.8 bolts under the situation of "nature fire," which means a temperature history including both heating and cooling phases. Kodur et al. [12], Hu et al. [13], Lange and Kawohl [14], and Moreno and Baddoo [15] studied the performance deterioration and failure mechanisms of high-strength bolts made of different materials (such as A325, A490, and stainless steel [16]) under fire. Ohlund et al. [17] discussed the physical properties of ultra-high-strength bolts at elevated temperatures from the perspective of microstructure. Using both steady-state and transient-state fire tests, Wang et al. [18] studied the shear behavior of lapped connections bolted by thread-fixed one-side bolts (TOB) at elevated temperatures. Fang et al. [19–21] investigated the robustness of steel-composite structures subject to localized fire and proposed a practical framework for robustness assessment. Santiago et al. [22] and Nadjai et al. [23] conducted natural fire tests of steel frames, and they studied the influence of connection types on failure modes and the influence of travelling fire on surrounding structures. Maraveas et al. [24] proposed an improved temperature-dependent constitutive model for steel to account for the local instabilities of slender plates in a fire situation.

The study on the mechanical properties of ordinary high-strength bolts under elevated temperatures has been extended from simple to complex stress states, and some high-performance (such as fire resistant) steels are beginning to get the attention of some scholars. Fire-resistant steel, by adding specific alloying elements (such as Cr, Mo, and Nb), can meet strength requirements at high temperatures (usually refers to 600°C) for a certain period of time (usually refers to 1~3 hours), thereby increasing the fire resistance ability and safety of buildings. In addition, fire-resistant steel can be used without spraying a fireproof coating or surface treatment. Compared with ordinary steel that require spraying a fireproof coating to achieve fire resistance, fire-resistant steel can avoid environmental issues caused by the coating peeling under long-term application. Sakumoto et al. [25] studied the high-temperature mechanical properties of high-strength fire-resistant bolts and the shear strength of friction joints using fire-resistant bolts. Ban et al. [26] compared the high-temperature mechanical properties of conventional high-strength grade 10.9 bolts and high-performance bolts produced by the Shougang Group Research Institute of Technology. They proposed constitutive models and prediction equations for describing the material properties of high-performance bolts at different temperatures. Li et al. [27, 28] conducted the material test of 20 MnTiB high-strength grade 10.9 bolts from room temperature to 700°C. According to the testing results, they obtained calculation models used for reduction coefficients of yield strength and the initial elastic modulus of ordinary high-strength bolts and fire-resistant high-strength bolts at high temperatures. Meng et al. [29] investigated the shear performance of bolted joints fabricated with BFRW10 high-strength fire-resistant bolts. They found that the failure mode of bolted joints changes from compressive failure on the bolt hole to shear failure of the bolt screw with increasing temperature.

Current studies have brought significant advances in finding the resistance to high temperatures of joints and connections fabricated with high-strength bolts. However, there is still a lack of research and relevant design methods on the mechanical properties of joints fabricated by fire-resistant steel and fire-resistant high-strength bolts under elevated temperatures or fire. Given the existing issues and lack of experimental data, this paper experimentally studies the mechanical performance of fire-resistant and high-strength bolted joints under the conditions of the room and elevated temperatures (20°C~700°C). Calculated models under different reliability degrees are proposed to predict the strength degradation of bolted joints (including fire-resistant and ordinary steel specimens) under elevated temperatures, which can provide a reference for the application of fire-resistant high-strength bolts and fire-resistant steel in practical engineering.

2. Experimental Program

2.1. Specimen Design. Figure 1 shows details of the specimen, which is the joint connected by high-strength bolts. The steel plate of the joint is made of fire-resistant steel Q460 produced by Shougang Group. The fire-resistant steel Q460 is manufactured through thermo-mechanical controlled processing (TMCP). Compared with ordinary steel processing, there are three points to be noted. (1) Alloying elements: it is necessary to properly add alloying elements (such as Cr and Mo), which are beneficial to the fire resistance of steel and strictly control the content of impurity elements (such as P and S). The chemical composition of the fire-resistant steel Q460 is shown in Table 1. (2) Rolling temperature: the beginning and final rolling temperatures of the fire-resistant steel Q460 in the recrystallized zone are 1150°C and 1120°C, respectively, while the beginning and final rolling temperatures in the unrecrystallized zone are 950°C and 850°C, respectively. (3) Cooling condition: an automatic control system, accelerated cooling control (ACC), is used to cool the fire-resistant steel Q460. The beginning and ending cooling temperatures are 780°C and 450°C, respectively, and the cooling rate is 20°C/s. After the heat preservation treatment at 600°C, Q460 is air-cooled.

The steel plate has only one type, which is fire resistant. Table 2 shows the mechanical behavior of a fire-resistant steel plate. The high-strength grade 10.9 bolts (M20) are used in the joints, which have two types, ordinary and fire-

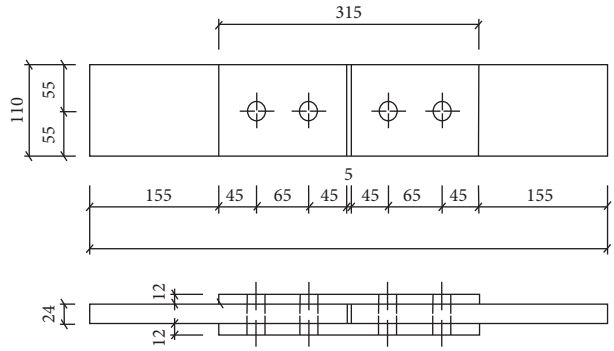

Figure 1: Schematic diagram of specimen details (unit: mm).

Table 1: Chemical composition of the fire-resistant steel Q460 (mass fraction (%)).

C	Si	Mn	P	S	Al	Ni + Cr + Cu	Nb + Ti + Mo	Fe
0.035	0.26	1.01	0.005	0.003	0.012	≤2.0	≤0.50	Bal

Table 2: Mechanical behavior the fire-resistant steel plate.

Thickness/ mm	$R_{p0.2}$ (MPa)	R_m (MPa)	Elongation A (%)	Yield-to-tensile strength ratio	180° cold-bending	Impact energy at −40°C Akv/J	Yield strength held at 600°C for 180 min (MPa)
10	490	636	23.5	0.77	$D = 3a$	353	345

Note. D is the diameter of the bending indenter and a is the thickness of the fire-resistant steel.

resistant, respectively. Table 3 shows the mechanical behavior of the fire-resistant and high-strength grade 10.9 bolt. Treatments of the friction surface between the steel plate and high-strength bolt have two types, which are impeller blasting and sprayed hard quartz sand. Both treatments are commonly used in practical engineering. The mechanical properties of high-strength bolted joints at elevated temperatures are investigated. Considering the maximum temperature (600°C~800°C) [23, 30] of locally directly heated members of a steel structure in a natural fire and the optimal temperature interval of the testing machine, five temperatures are chosen, which are 20°C (room temperature), 200°C, 400°C, 600°C, and 700°C. Table 4 shows the experimental condition and parameters of each specimen. The experiment with each conditional parameter is repeated twice, and the total quantity of specimens is 40 (including 8 specimens at room temperature and 32 specimens at elevated temperatures).

2.2. Configuration and Measurements during Testing. All 40 specimens were tested in the MTS high-temperature testing machine (see Figure 2), which has a loading capacity of 1000 kN in the Key Laboratory of Tongji University. The steady-state test of elevated temperature is carried out. The temperature is controlled by the electric-heating furnace, which is supported by intelligent temperature control equipment. The electric-heating furnace can be controlled according to a given temperature curve. The highest temperature can reach 1000°C, and the maximum heating rate is 30°C/min. The testing machine is equipped with an extensometer to continuously measure the displacement of the specimen.

2.3. Experimental Procedure. According to the current code [31, 32] of fire resistance tests, the experimental procedure is as follows:

(1) Installation of high-strength bolts: first, for the convenience, high-strength bolts of the specimen are initially screwed with an ordinary wrench. Then, we tighten it with a torque wrench to complete the installation. The pretightening force of a high-strength bolt is controlled and recorded by the axial-force detector. The pretightening force of a high-strength grade 10.9 bolt (M20) should be 155 kN.

(2) The assembled specimen is installed in the electric-heating furnace of the testing machine, and the center of the specimen is completely aligned with the center of the fixed position (see Figure 2) of the testing machine. The specimen is heated to the specified temperature and kept at a constant temperature for 60 min.

(3) After the surface temperature of the specimen is stabilized, the specimen is loaded, and the loading force and displacement data are collected and recorded in real time.

(4) The loading process is ended when the loading force is reduced to less than 85% of the ultimate bearing capacity.

Table 3: Mechanical behavior of the fire-resistant and high-strength grade 10.9 bolt.

Size	$R_{p0.2}$ (MPa)	R_m (MPa)	Elongation A (%)	Area reduction (%)	Rockwell hardness HRC	Impact energy at room temperature Akv/J	Yield strength held at 600°C for 180 min (MPa)
M20	1041	1075	21.5	66	35.2	152	513

Table 4: Experimental condition and parameters of the specimens.

Specimen number	Temperature	Treatment of friction surface	Type of high-strength bolts (Grade 10.9 M20)	Specimen quantity
A1	Room temperature (20°C)	Impeller blasting	Fire resistant	2
A2			Ordinary	2
A3		Sprayed hard quartz sand	Fire resistant	2
A4			Ordinary	2
B1	200°C	Impeller blasting	Fire resistant	2
B2			Ordinary	2
B3		Sprayed hard quartz sand	Fire resistant	2
B4			Ordinary	2
C1	400°C	Impeller blasting	Fire resistant	2
C2			Ordinary	2
C3		Sprayed hard quartz sand	Fire resistant	2
C4			Ordinary	2
D1	600°C	Impeller blasting	Fire resistant	2
D2			Ordinary	2
D3		Sprayed hard quartz sand	Fire resistant	2
D4			Ordinary	2
E1	700°C	Impeller blasting	Fire resistant	2
E2			Ordinary	2
E3		Sprayed hard quartz sand	Fire resistant	2
E4			Ordinary	2

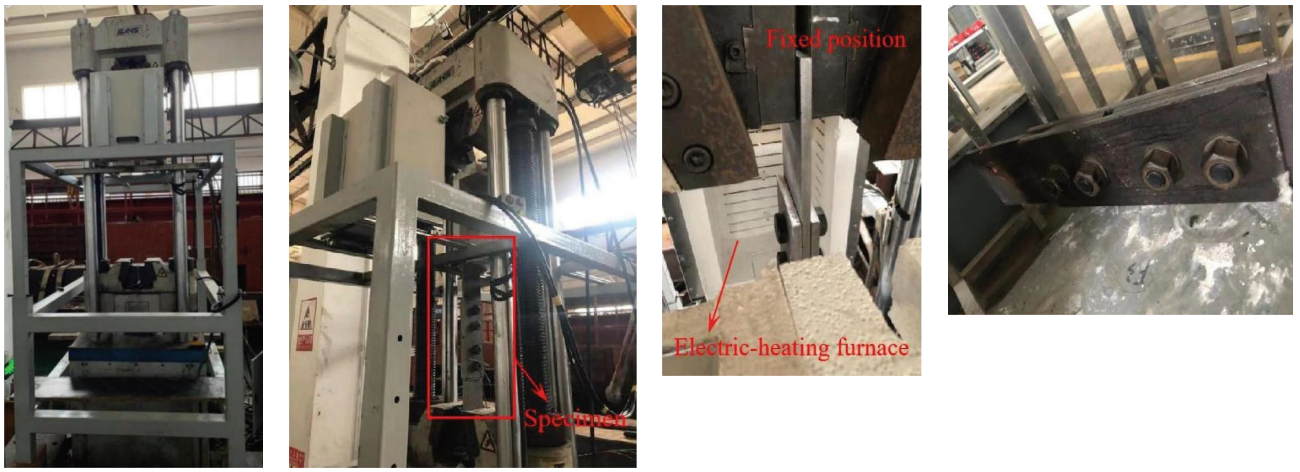

(a) (b) (c) (d)

Figure 2: MTS high-temperature testing machine and the specimen at elevated temperatures. (a) A testing machine. (b) Installation of the specimen. (c) Local details. (d) Details of the specimen.

(5) When the temperature in the furnace falls below 200°C, we open the furnace to cool down. We replace the specimen when the surface temperature is less than 50°C.

3. Analysis of Experimental Results

3.1. Failure Mode. Figure 3 shows the failure mode of ordinary high-strength bolt specimens. Under room

temperature, the bolt in the specimen almost has no shear deformation (see Figure 3(a)), but the bolt hole of the fire-resistant steel plate has significant deformation, which shows that the final failure mode is the compressive failure of the bolt hole wall. Under the condition of 200°C~600°C, both the bolt hole and screw have large plastic deformation under the external loading (see Figure 3(b)). The steel plate and bolt share the shear force, and the shear deformation degree of the screw is smaller than that of the bolt hole. At 700°C, there is almost no deformation of the bolt hole, but the shear deformation of the screw is significant (see Figure 3(c)). Thus, the final failure mode of the specimen is a double shear failure of the bolt screw. For the joint connected by ordinary high-strength bolts and a fire-resistant steel plate, the higher the temperature is, the more likely the failure is to occur on the bolt.

Figure 4 shows the failure mode of fire-resistant high-strength bolt specimens. Under the condition of 20°C~700°C, all specimens have the same failure mode, which is the compressive failure of the bolt-hole wall. The bolt hole experiences significant plastic deformation, while the deformation of the screw is not significant.

3.2. Load-Deformation Relationships. Figure 5 shows the relationship between loading force and displacement of specimens under different experimental conditions. According to this figure, there are four stages during the whole loading process (shown in Figure 5(a)). (1) Stage 1 is the initial elastic stage. In this stage, the loading force of the specimen nearly increases linearly with the increase in displacement. There is no contact between the bolt screw and bolt hole wall, and thus, the bearing capacity of the specimen mainly depends on the friction between the bolt and the steel plate. (2) Stage 2 has slip characteristics. At this stage, relative slip displacement occurs between the bolt and steel plate. This is the reason that the loading force-displacement curve appears to have a significant platform segment or descending segment. (3) Stage 3 corresponds to the extrusion-strengthening stage. At this stage, the bolt is in close contact with the bolt hole wall. The hole wall is under pressure, the bolt screw is under shear, and the loading force increases again with the increase in displacement. As can be seen from the figure, under the same deformation condition, strength and stiffness (slope of the curve) of the specimen decrease with the increase of temperature, which indicates that the "strengthening" effect tends to weaken. (4) Stage 4 corresponds to the period from the ultimate strength (F_N) to the failure of the specimen. At this stage, the slope of the loading force-displacement curve begins to decline, and both material strength and specimen deformation reach the limit state.

3.3. Degradation of Deformation Capacity. The ultimate displacement Δ_N is defined as the displacement when the specimen reaches ultimate strength (see Figure 6(a)), which represents the ductility and deformation capacity of the specimen to some extent. Figure 6 shows the relationship between ultimate displacement and temperature. Different treatments of friction surfaces (specifically, impeller blasting and sprayed hard quartz sand) almost have no obvious effect on the Δ_N. For both ordinary bolt specimens and fire-resistant bolt specimens, Δ_N generally shows a trend of decreasing with the increase of temperature. In case of the temperature from 20°C to 400°C, Δ_N of ordinary bolt specimens and that of fire-resistant bolt specimens are similar and do not show obvious regularity. When the temperature is between 400°C and 700°C, the decreasing rate of Δ_N of ordinary bolt specimens is faster than that of fire-resistant bolt specimens. As a result, Δ_N of fire-resistant bolt specimens is even 1.5 times as much as high of ordinary bolt specimens at 700°C. This result is related to the failure mode of specimens (see Section 3.1). The ordinary bolt specimens show the double shear failure of a bolt screw at elevated temperatures (such as 600°C and 700°C), and the fire-resistant steel plate cannot contribute its plastic deformation ability. The specimen deformation mainly comes from the very limited shear deformation of high-strength bolts, and thus, Δ_N is significantly small.

3.4. Degradation of Bearing Capacity. Table 5 shows the experimental results of specimen bearing capacity. The ultimate strength (F_N) and slip load (F_S) of specimens correspond to the beginning points of Stage 2 and Stage 4 (see Section 3.2 and Figure 5(a)), respectively. To facilitate comparison, F_N and F_S are standardized. Taking the ultimate strength of specimens at room temperature ($F_{N,20}$) as a reference, the reduction factor of the tensile strength (K_N) is calculated, where $K_N = F_{N,T}/F_{N,20}$. $F_{N,T}$ is the ultimate strength of specimens at elevated temperatures, whose treatment of the friction surface and type of high-strength bolts are the same as the corresponding specimen at room temperature. Similarly, the reduction factor of the slip strength (K_S) is calculated, where $K_S = F_{S,T}/F_{S,20}$. $F_{S,T}$ and $F_{S,20}$ are the slip loads of specimens at elevated temperatures and room temperature, respectively.

Figure 7 shows the relationship of K_N and temperature. For the specimens of both ordinary and fire-resistant bolts, the reduction factor of tensile strength (K_N) decreases with the increase in temperature. In addition, different treatments of the friction surface almost have no effect on the K_N. For specimens of ordinary bolts, when the temperature is less than 400°C, K_N decreases slowly with the increase in temperature. When the temperature reaches 400°C, K_N decreases to 0.9 times the original value (20°C). As the temperature exceeds 400°C, K_N decreases rapidly. At 600°C, K_N decreases to below 0.4, and K_N is only 0.2 at 700°C, indicating that the specimen has lost most of its bearing capacity. For specimens of fire-resistant bolts, K_N of them is always larger than that of ordinary bolt specimens. Similar to specimens of ordinary bolts, K_N of fire-resistant bolts specimens decreases slowly from 20°C to 400°C, and there is little difference between K_N of ordinary bolt specimens and K_N of fire-resistant bolt specimens. When the temperature is between 400°C and 700°C, K_N of fire-resistant bolt specimens decreases relatively rapidly, and the rate of decline is smaller than that of ordinary bolt specimens. For K_N of fire-resistant

(a) (b) (c)

Figure 3: Failure of ordinary high-strength bolt specimens. (a) A4. (b) B4. (c) E2.

(a) (b) (c) (d)

Figure 4: Failure of fire-resistant high-strength bolt specimens. (a) A3. (b) C3. (c) D3. (d) E1.

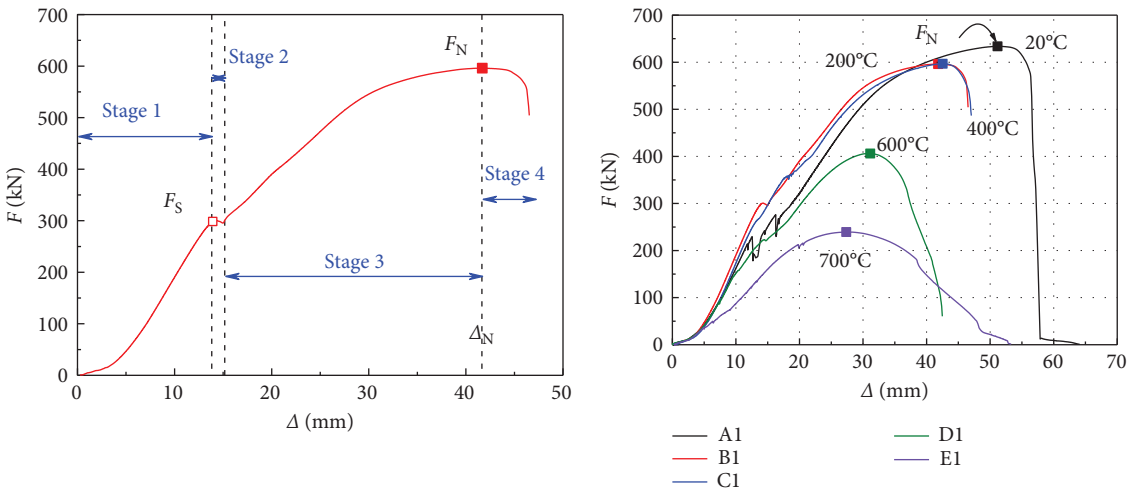

(a) (b)

Figure 5: Continued.

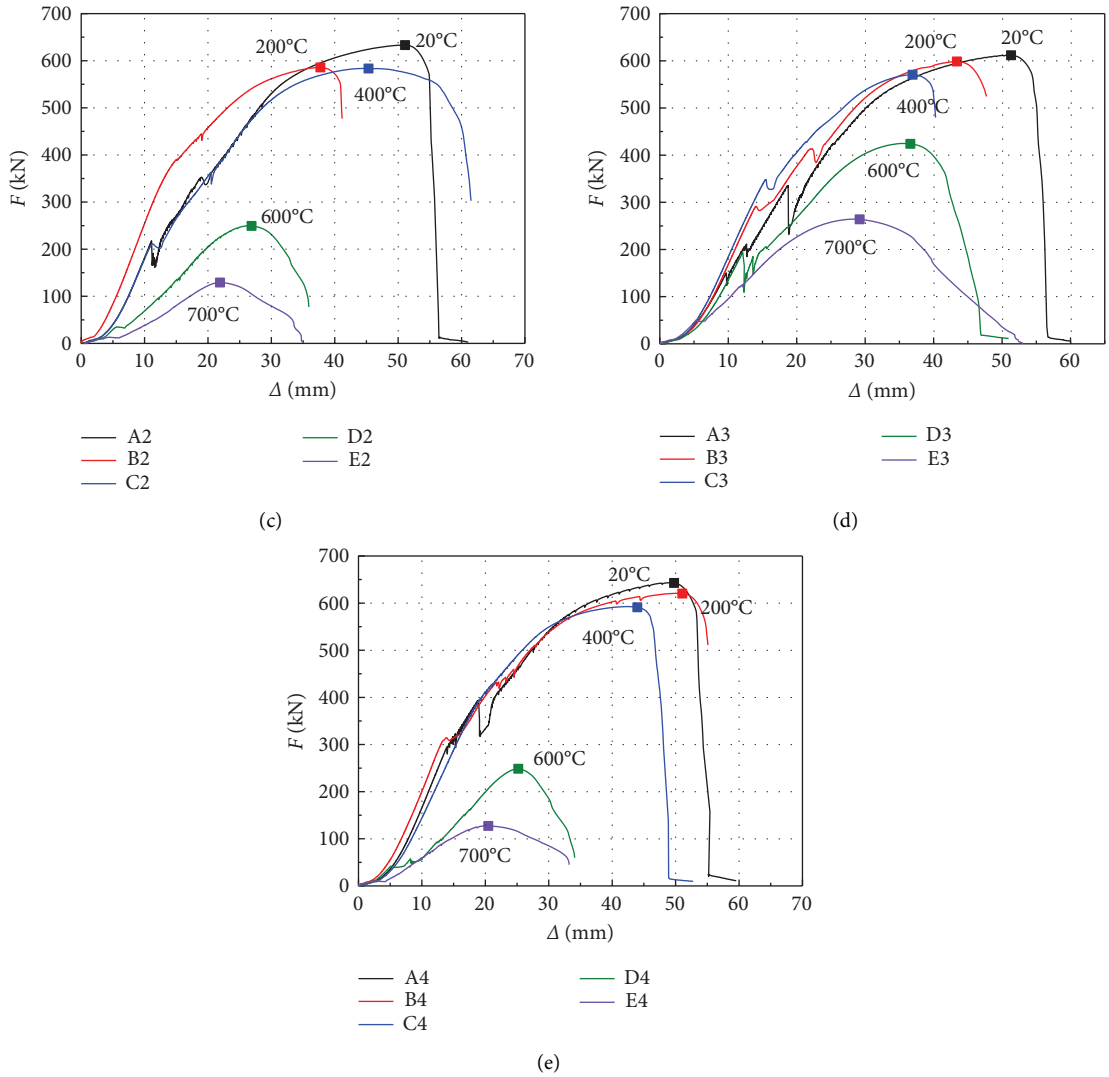

Figure 5: The relationship between loading force and displacement of specimens. (a) B1. (b) Impeller blasting and fire-resistant bolts. (c) Impeller blasting and ordinary bolts. (d) Sprayed hard quartz sand and fire-resistant bolts. (e) Sprayed hard quartz sand and ordinary bolts.

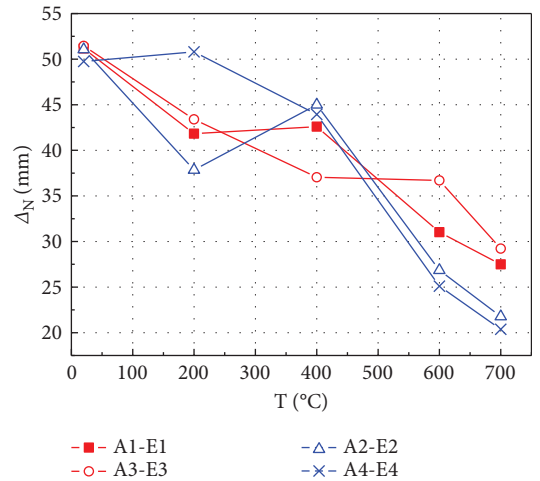

Figure 6: The relationship between ultimate displacement and temperature.

Table 5: Experimental results of specimen bearing capacity.

Type of high-strength bolts	Specimen numbers	Temperature T (°C)	F_N (kN)	K_N	F_S (kN)	K_S
Fire resistant	A1	20	633.70	1.00	229.70	1.00
	B1	200	593.60	0.94	363.55	1.58
	C1	400	603.15	0.95	332.60	1.45
	D1	600	411.10	0.65	102.65	0.45
	E1	700	249.30	0.39	33.60	0.15
	A3	20	611.80	1.00	150.2	1.00
	B3	200	604.80	0.99	281.25	1.87
	C3	400	562.75	0.92	324.55	2.16
	D3	600	428.00	0.70	186.45	1.24
	E3	700	258.85	0.42	47.45	0.32
Ordinary	A2	20	633.10	1.00	218.10	1.00
	B2	200	595.40	0.94	370.80	1.70
	C2	400	581.20	0.92	226.60	1.04
	D2	600	241.50	0.38	34.75	0.16
	E2	700	128.45	0.20	12.55	0.06
	A4	20	643.30	1.00	295.10	1.00
	B4	200	622.05	0.97	316.10	1.07
	C4	400	592.60	0.92	420.80	1.43
	D4	600	229.40	0.36	36.00	0.12
	E4	700	125.95	0.20	9.90	0.03

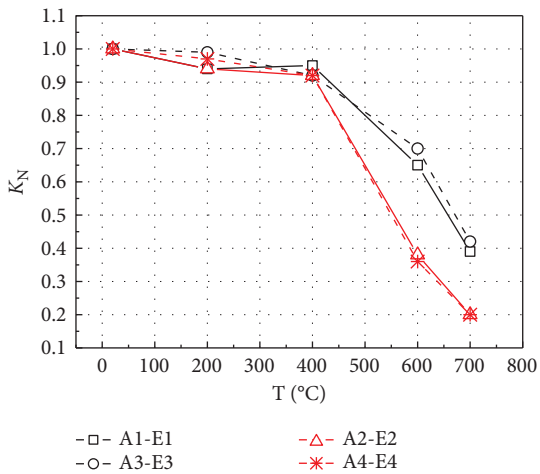

Figure 7: The relationship between K_N and temperature.

bolt specimens, it is about 0.7 at 600°C and 0.4 at 700°C, which is far greater than that of ordinary bolt specimens. The abovementioned results remind us that when the design temperature is greater than 400°C, there is a great difference between the properties of ordinary and fire-resistant bolted joints. Therefore, in this case, the performance matching of connecting members should be considered, such as the connecting bolts of fire-resistant steel plates, which should also be made of fire-resistant steel.

Figure 8 shows the relationship between K_S and temperature. For both ordinary bolt specimens and fire-resistant bolt specimens, the reduction factor of slip strength (K_S) shows a trend of increasing first (20°C~400°C) and then decreasing (400°C~700°C). When the temperature exceeds 400°C, K_S decreases sharply, and the specimen has almost no slip load at 700°C. Different treatments of friction surfaces (specifically, impeller blasting and sprayed hard quartz sand) have a visible influence on K_S, especially on fire-resistant bolt specimens. Under the same treatment of the friction surface, K_S of fire-resistant bolt specimens is always larger than that of ordinary bolt specimens.

Considering the abovementioned analysis of the experimental results of bearing capacity degradation with temperature, in cases where the temperature is less than 400°C, fire-resistant and high-strength bolted joints can be designed according to the friction type connection. In cases where the temperature is greater than 400°C, fire-resistant and high-strength bolted joints are suggested not to consider the slip bearing capacity and to be designed according to the shear bearing type connection.

3.5. Calculation Model of Reduction Factor. The reduction factor of tensile strength plays an important role in evaluating the bearing capacity of components, joints, and structures under elevated temperature and fire conditions. Based on the relationship between K_N and temperature in the experimental results, the calculated model of K_N is proposed in linear form (equation (1)), which is convenient for application and structural design. Equations (2) and (3) are calculated models of K_N for specimens of fire-resistant bolts and for specimens of ordinary bolts, respectively. The parameters a and b in the calculated model are obtained by fitting. The degrees of fitting of equation (2) are $R = 0.842$ ($20°C \le T < 400°C$) and $R = 0.976$ ($400°C \le T < 700°C$), respectively. The degrees of fitting of equation (3) are $R = 0.912$ ($20°C \le T < 400°C$) and $R = 0.994$ ($400°C \le T < 700°C$), respectively. Figure 9(a) shows experimental and calculated reduction factors K_N plotted with respect to temperatures.

The degree of reliability of the calculated model (equations (2) and (3)) obtained by fitting the experimental data is 50%, and the probability of the predicted K_N being larger or smaller than the actual value is almost the same, which is logically unsafe. The large degree of reliability

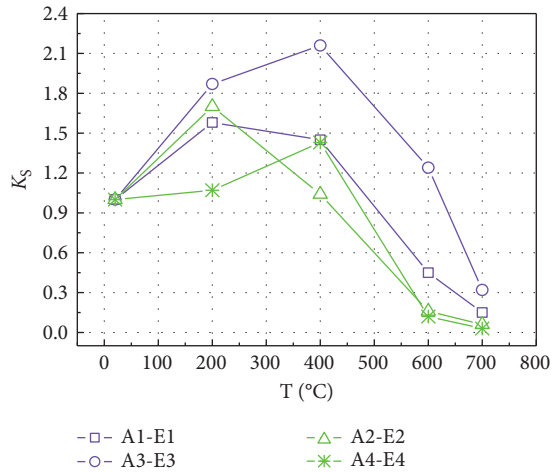

Figure 8: The relationship between K_S and temperature.

indicates the great probability that the actual K_N is greater than the calculated K_N. In practical engineering, the calculated model of K_N with larger reliability is usually required for safety. K_N is a variable between 0 and 1, so it is assumed to satisfy the log-normal distribution. The estimated value of b with the degree of reliability p_j is expressed in equations (4) and (5). Table 6 shows the model parameters of K_N under different degrees of reliability, which can be selected for the suitable reliability according to requirements. Figure 9(b) shows the calculated model of K_N for fire-resistant high-strength bolt specimens under different reliability levels (including 50%, 85%, 95%, and 99%), and Figure 9(c) shows the calculated model of K_N for ordinary high-strength bolt specimens under different reliability levels:

$$K_N = aT + \hat{b}, \tag{1}$$

$$K_N = \begin{cases} -0.000167T + 1.012, & 20℃ \le T < 400℃ \\ -0.0017T + 1.6252, & 400℃ \le T < 1000℃ \end{cases} \text{for specimens of fire} - \text{resistant bolts}, \tag{2}$$

$$K_N = \begin{cases} -0.00022T + 1, & 20℃ \le T < 400℃ \\ -0.00245T + 1.892, & 400℃ \le T < 1000℃ \end{cases} \text{for specimens of or di nary bolts}, \tag{3}$$

$$\hat{b} = \overline{b} + \mu_{pj} s, \tag{4}$$

$$s = \sqrt{\frac{1}{n-1} \sum_{i=1}^{n} \left(K_{Ni} - \overline{K}_N\right)^2}, \tag{5}$$

where a and b are model parameters of the linear calculated model, $\hat{b}$ and $\overline{b}$ are estimated value and average value of b, respectively, μ_{pj} is the standard normal deviator (where subscript pj represents j degrees of reliability), s is the standard deviation of experimental specimens, $\mu_{pj}s$ is the model error of the linear calculated model, n is the total quantity of specimens, K_{Ni} is the reduction factor of each specimen, and $\overline{K}_N$ is the calculated reduction factor based on the model parameter $\overline{b}$.

Figure 10 shows the comparison between experimental and calculated reduction factors of tensile strength. The solid line is the 1 : 1 line, two dash lines are bounds that correspond to the scatter band of 1.05, and two dot lines are bounds that correspond to the scatter band of 1.15. Most calculated reduction factors are located within a safe scatter band of 1.05. All calculated reduction factors are located within a scatter band of 1.15, which shows good accuracy of the proposed calculated model. The proposed linear model has relatively great convenience for application and reliability design, and considering the limited experimental data, more work can be carried out to have a solid guideline.

Figure 11 shows an illustrative design example. In a steel-braced frame, a beam is usually connected to the cantilever arm of a column by connecting plates and bolts,

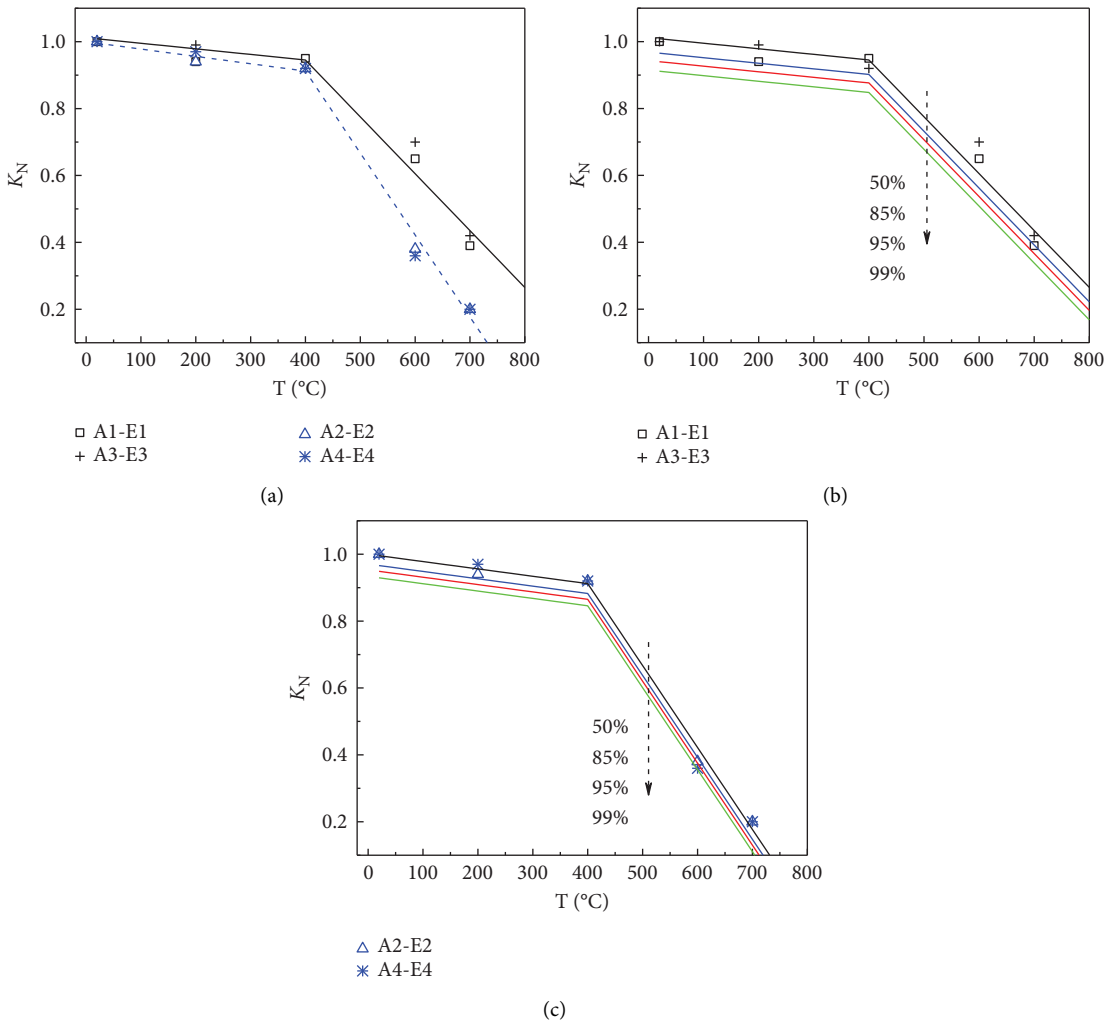

Figure 9: (a) Calculated model of K_N. (b) Calculated model of K_N for fire-resistant high-strength bolt specimens under different reliability. (c) Calculated model of K_N for ordinary high-strength bolt specimens under different reliabilities.

Table 6: The model parameters of K_N under different degrees of reliability.

Degrees of reliability (p_j)			50%	85%	95%	99%
$\widehat{b}$	μ_{pj}		0	−1.036	−1.645	−2.326
	Specimens of fire-resistant bolts	20°C ≤ T < 400°C	1.012	0.9687	0.9433	0.9149
		400°C ≤ T < 700°C	1.6252	1.5819	1.5565	1.5281
	Specimens of ordinary bolts	20°C ≤ T < 400°C	1	0.9705	0.9532	0.9338
		400°C ≤ T < 700°C	1.892	1.8625	1.8452	1.8258

Note. μ_{pj} corresponds to each reliability and P_j is obtained from the table of the standard normal deviator.

which is a typical beam-column connection. As shown in this figure, the force conditions of connecting plates and bolts in the flange connection are the same as those in the bolted joint of this paper experiment. Using the proposed prediction model of K_N, the design value of high temperature bearing capacity at the flange connection can be obtained for a given temperature, bolt type, and reliability. In addition, this calculated process and example can be applied to structures of other steel types (such as stainless steel) for fire design.

In addition, material reduction factors and experimental results are compared, which is shown in Figure 12. Equations (6) and (7) [26] are the calculated model of high-strength fire-resistant bolt (represented by $K_{N,FRB}$) and an ordinary high-strength bolt (represented by $K_{N,B}$), respectively. They are obtained from a summary of experimental data on high-strength bolts (including fire-resistant bolts and ordinary bolts) at elevated temperatures in recent 20 years. The illustration of samples in the experiment is shown in Figure 12. Equation (8) [33] is the calculated model of fire-

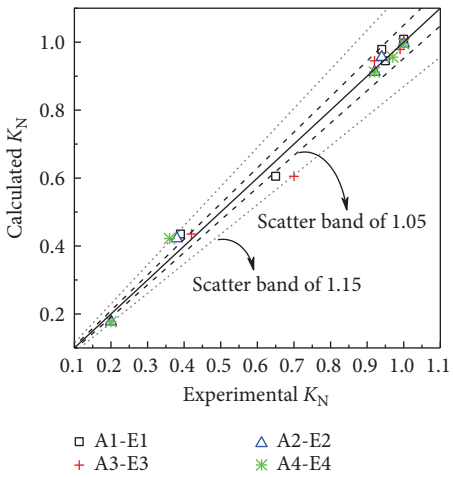

Figure 10: Comparison of experimental and calculated reduction factors of tensile strength.

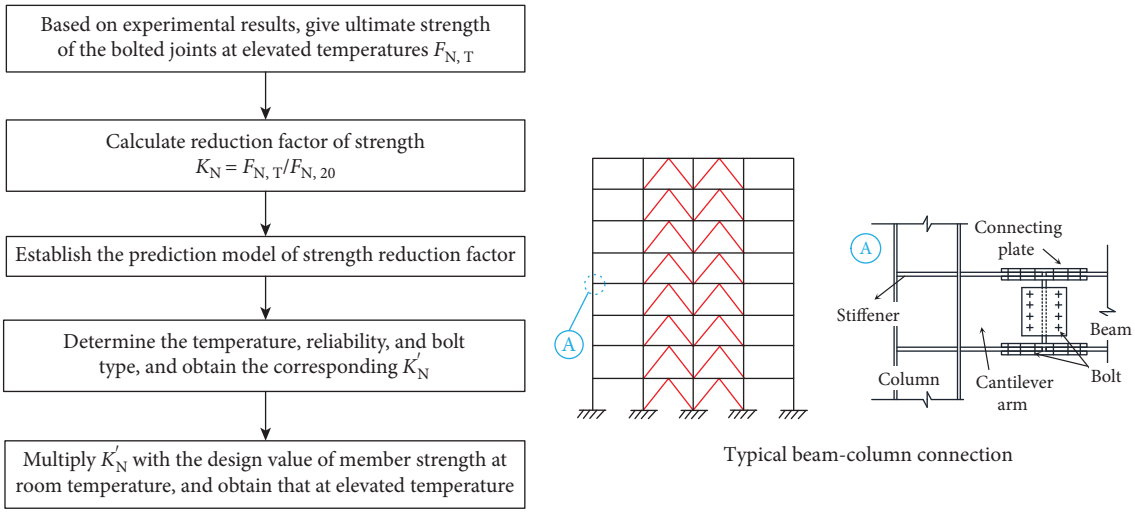

Figure 11: An illustrative design example.

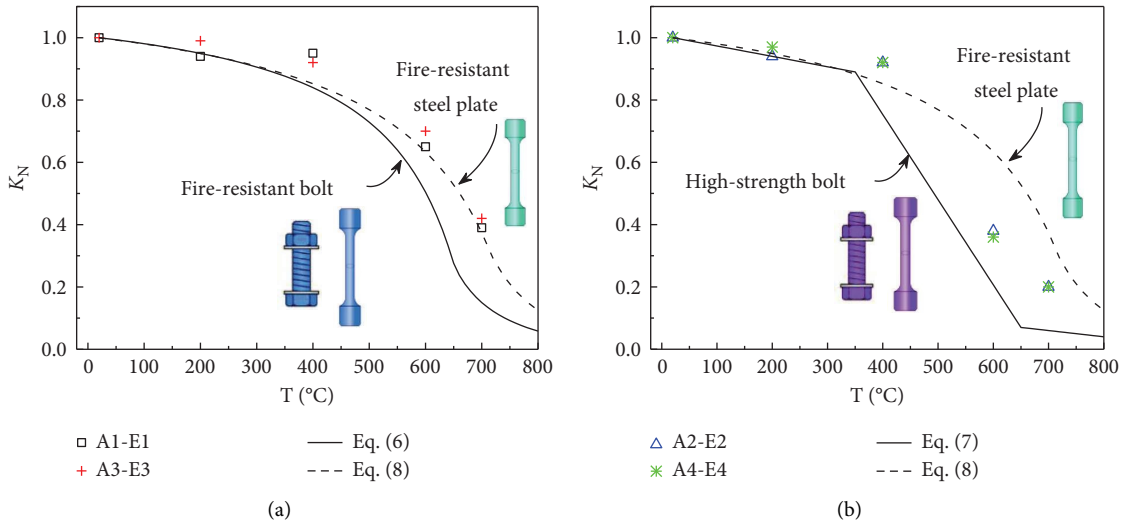

Figure 12: Comparison of material reduction factor and experimental results. (a) Specimens of fire-resistant high-strength bolts. (b) Specimens of ordinary high-strength bolts.

resistant steel (represented by $K_{N,FRP}$). For specimens (bolted joints in this study) of fire-resistant bolts, $K_{N,FRP}$ is closer to the experimental results. This result is related to the failure mode of the specimens (whose fire-resistant bolts are almost not damaged). For specimens of ordinary high-strength bolts, in the case of 400°C~700°C, $K_{N,FRP}$ overestimates the experimental results and $K_{N,B}$ underestimates the experimental results. This result is related to the change in failure mode of ordinary high-strength bolt specimens (see Section 3.1) under elevated temperatures. The mechanical properties of bolt material and steel material are different at high temperatures, and the actual force of a bolted joint is complicated. Thus, there may be a calculated error if the reduction factor of the material is directly used to evaluate the mechanical properties of bolted joints, and the damage state should be taken into consideration (especially in cases of elevated temperatures):

$$K_{N,FRB} = \begin{cases} \dfrac{7T - 4790}{6T - 4770}, & 20℃ \le T < 650℃, \\ \dfrac{7(1000 - T)}{100(T - 560)}, & 650℃ \le T < 1000℃, \end{cases} \tag{6}$$

$$K_{N,B} = \begin{cases} 1 - \dfrac{T - 20}{3000}, & 20℃ \le T \le 350℃, \\ 1.792 - \dfrac{41(T - 20)}{15000}, & 350℃ < T \le 650℃, \\ 0.196 - \dfrac{T - 20}{5000}, & 650℃ < T \le 1000℃, \end{cases} \tag{7}$$

$$K_{N,FRP} = \begin{cases} \dfrac{6(T - 768)}{5(T - 918)}, & 20℃ \le T < 700℃, \\ \dfrac{1000 - T}{8(T - 600)}, & 700℃ \le T \le 1000℃. \end{cases} \tag{8}$$

4. Conclusion

Experiments on 40 specimens of high-strength and fire-resistant bolted joints are conducted. The experimental results are used to investigate the effect of temperature, treatment of the friction surface, and steel type of a high-strength bolt on the mechanical performance of specimens. A calculation model is proposed to predict the reduction factor of tensile strength. The main findings and conclusions are summarized as follows:

(1) The bearing and deformation capacities of fire-resistant bolt specimens are generally better than those of ordinary bolt specimens at elevated temperatures, especially when the temperature exceeds 400°C. As the temperature increases, the failure mode of ordinary bolt specimens changes from a compressive failure of the bolt hole wall (20°C~400°C) to a double shear failure of the bolt screw (>600°C). The fire-resistant bolt specimens have the same failure mode (which is the compressive failure of the bolt hole wall) under the condition of 20°C~700°C.

(2) The effect of different treatments of the friction surface (specifically, impeller blasting and sprayed hard quartz sand) on the ultimate displacement and ultimate strength of specimens can be negligible. However, the treatments of the friction surface have a relatively significant effect on the slip load of specimens.

(3) The fire-resistant and high-strength bolted joints can be designed according to the friction type of connection when the temperature is between 20°C~400°C. In case of the temperature greater than 400°C (400°C~700°C), fire-resistant and high-strength bolted joints are suggested to be designed according to the shear bearing type connection.

(4) For both ordinary and fire-resistant bolt specimens, the reduction factor of tensile strength (K_N) decreases with the increase in temperature. K_N decreases slowly when the temperature is less than 400°C, and in the case of 400°C, K_N is 0.9~0.95 times the value at 20°C. As the temperature exceeds 400°C, K_N decreases rapidly. K_N of ordinary and fire-resistant bolt specimens at 700°C are about 0.2 and 0.4, respectively, indicating that the specimen has lost most of its bearing capacity.

(5) The calculated model of K_N under different degrees of reliability is proposed to predict the tensile strength of bolted joints (including fire-resistant and ordinary high-strength bolted specimens) under elevated temperatures, which has the potential to be used for the fire-resistant design of connections and structures. At 20°C~400°C, K_N of fire-resistant and ordinary high-strength bolted specimens is similar, and K_N of fire-resistant bolt specimens is larger than that of ordinary bolt specimens under the condition of 400°C~700°C.

According to the results in this study, it is necessary to use fire-resistant bolts to connect fire-resistant steel plates. The prediction models of the strength reduction factor for fire-resistant steel plates matched with different types of bolts are proposed for reference in structural fire design. The abovementioned study is helpful in understanding and promoting the application of fire-resistant steel, especially in a country like China, where fire-resistant steel is not widely used. Given the better practical significance, we prepare to conduct an experimental study on the joint of ordinary steel plates and fire-resistant high-strength bolts to consider the influence of the type of steel plate on the mechanical properties of bolted joints at elevated temperatures.

Data Availability

The experimental data used to support the findings of this study are currently under embargo while the research findings are commercialized. The data, 6 months after

publication of this article, can be obtained from the corresponding author upon request.

Conflicts of Interest

The authors declare that they have no conflicts of interest.

Acknowledgments

The authors gratefully acknowledge the financial support from the National Key Research and Development Program of China (no. 2018YFC0705500).

References

[1] J. Lyu, Q. Chen, H. Xue, Y. Cai, J. Lyu, and S. Zhou, "Fire resistance of composite beams with restrained superposed slabs," *Advances in Materials Science and Engineering*, vol. 2020, Article ID 7109382, 13 pages, 2020.

[2] Z. Fang, K. Roy, H. Liang et al., "Numerical simulation and design recommendations for web crippling strength of cold-formed steel channels with web holes under interior-one-flange loading at elevated temperatures," *Buildings*, vol. 11, no. 12, p. 666, 2021.

[3] F. Liu, X. Wang, B. Cai, X. Li, and L Yang, "Mechanical performance analysis of steel beam-column joints in fabricated multirise steel structures after fire," *Journal of Chemistry*, vol. 2022, Article ID 7425801, 8 pages, 2022.

[4] R. M. Lawson, "Behavior of steel beam-to-column connections in fire," *Structural Engineer*, vol. 68, no. 14, 1990.

[5] L. Chen and Y. C. Wang, "Methods of improving survivability of steel beam/column connections in fire," *Journal of Constructional Steel Research*, vol. 79, pp. 127–139, 2012.

[6] Y. Theodorou, "Mechanical Properties of Grade 8.8 Bolts at Elevated Temperatures," MSc Dissertation, University of Sheffield, Sheffield, UK, 2001.

[7] P. A. Król and M. Wachowski, "Effect of fire temperature and exposure time on high-strength steel bolts microstructure and residual mechanical properties," *Materials*, vol. 14, no. 11, p. 3116, 2021.

[8] J. Lange and F. González, "Behavior of high-strength grade 10.9 bolts under fire conditions," *Structural Engineering International*, vol. 22, no. 4, pp. 470–475, 2012.

[9] G. Lou, M. C. Zhu, M. Li, C. Zhang, and G. Q. Li, "Experimental research on slip-resistant bolted connections after fire," *Journal of Constructional Steel Research*, vol. 104, pp. 1–8, 2015.

[10] M. Zhu, Y. J. Jiang, G. B. Lou, and G. Q. Li, "Test on slip coefficient of high-strength bolted slip-critical connections after fire," *Applied Mechanics and Materials*, vol. 351-352, no. 351-352, pp. 1368–1371, 2013.

[11] F. Hanus, G. Zilli, and J. M. Franssen, "Behaviour of grade 8.8 bolts under natural fire conditions: tests and model," *Journal of Constructional Steel Research*, vol. 67, no. 8, pp. 1292–1298, 2011.

[12] V. Kodur, S. Kand, and W. Khaliq, "Effect of temperature on thermal and mechanical properties of steel bolts," *Journal of Materials in Civil Engineering*, vol. 24, no. 6, pp. 765–774, 2012.

[13] Y. Hu, J. B. Davison, I. W. Burgess, and F. Liu, "Comparative Study of the Behavior of the BS4190 and BS EN ISO 4014 Bolts in fire," in *Proceedings of the 3rd International Conference on Steel and Composite Structure*, Manchester, UK, 2007.

[14] J. Lange and A. Kawohl, "Tension-shear interaction of high-strength bolts during and after fire," *Steel Construction*, vol. 12, no. 2, pp. 124–134, 2019.

[15] E. N. Moreno and N. R. Baddoo, *Stainless Steel in Fire*, The Steel Construction Institute, Silwood Park, UK, 2007.

[16] M. A. Shaheen, S. Afshan, and A. S. J. Foster, "Performance of axially restrained carbon and stainless steel perforated beams at elevated temperatures," *Advances in Structural Engineering*, vol. 24, no. 15, pp. 3564–3579, 2021.

[17] C. E. I. C. Ohlund, M. Lukovic, J. Weidow, M. Thuvander, and S. E. Offerman, "A comparison between ultra-high-strength and conventional high-strength fastener steels: mechanical properties at elevated temperature and microstructural mechanisms," *ISIJ International*, vol. 56, no. 10, pp. 1874–1883, 2016.

[18] P. Wang, Y. You, Q. Xu, Q. Wang, and F. Liu, "Shear behavior of lapped connections bolted by thread-fixed one-side bolts at elevated temperatures," *Fire Safety Journal*, vol. 125, Article ID 103415, 2021.

[19] C. Fang, B. A. Izzuddin, A. Y. Elghazouli, and D. Nethercot, "Robustness of steel-composite building structures subject to localised fire," *Fire Safety Journal*, vol. 46, no. 6, pp. 348–363, 2011.

[20] C. Fang, B. A. Izzuddin, A. Y. Elghazouli, and D. Nethercot, "Robustness of multi-storey car parks under localised fire—towards practical design recommendations," *Journal of Constructional Steel Research*, vol. 90, pp. 193–208, 2013.

[21] C. Fang, B. A. Izzuddin, R. Obiala, A. Elghazouli, and D. Nethercot, "Robustness of multi-storey car parks under vehicle fire," *Journal of Constructional Steel Research*, vol. 75, pp. 72–84, 2012.

[22] A. Santiago, L. Simoes da Silva, G. Vaz, P. Vila Real, and A. G. Lopes, "Experimental investigation of the behaviour of a steel sub-frame under a natural fire," *Steel and Composite Structures*, vol. 8, no. 3, pp. 243–264, 2008.

[23] A. Nadjai, A. Naveed, M. Charlier et al., "Large scale fire test: the development of a travelling fire in open ventilation conditions and its influence on the surrounding steel structure," *Fire Safety Journal*, vol. 130, Article ID 103575, 2022.

[24] C. Maraveas, T. Gernay, and J. M. Franssen, "An equivalent stress method to account for local buckling in beam finite elements subjected to fire," *Journal of Structural Fire Engineering*, vol. 10, no. 3, pp. 340–353, 2019.

[25] Y. Sakumoto, K. Keira, F. Furumura, and T. Ave, "Tests of fire-resistant bolts and joints," *Journal of Structural Engineering*, vol. 119, no. 11, pp. 3131–3150, 1993.

[26] H. Y. Ban, Q. M. Yang, Y. J. Shi, and Z. Luo, "Constitutive model of high-performance bolts at elevated temperatures," *Engineering Structures*, vol. 233, Article ID 111889, 2021.

[27] L. Guoqiang, M. Li, Y. Yin, and S. Jiang, "Experimental studies on the behavior of high-strength bolts made of 20MnTiB steel at elevated temperatures," *China Civil Engineering Journal*, vol. 34, no. 5, pp. 100–104, 2001.

[28] L. Guoqiang, L. Han, and G. Lou, *Fire Resistance Design of Steel Structure and Steel-concrete Composite Structure*, pp. 93–114, China Construction Industry Press, Beijing, China, 2006.

[29] L. Meng, C. Tu, Y. Shi, and Y. Wu, "Experimental study on shear performance of high-strength bolted connections fabricated from high-performance fire-resistant steel at elevated temperature," *Journal of Building Structures*, vol. 42, no. 06, pp. 85–93, 2021.

[30] R. Shi-Peng, Z. Jin-cheng, and S. Zhen-sen, D. Li-Ping, Research on fire resistance test of a steel frame building under

spreading fire," *Journal of Building Structures*, vol. 43, no. 09, pp. 103–114, 2022.

[31] British Standards Institution, *Euro Code 3: Design of Steel Structures: Part 1.2: Structural Fire Design: BSEN1993-1-1*, British Standards Institution, London, UK, 2004.

[32] Chinese Standards, *Fire Resistance Tests-Elements of Building Construction: GB/T 9978.2-2019*, Chinese Standards, Beijing, China, 2019.

[33] China Construction Industry, *Code for Fire Safety of Steel Structures in Buildings GB51249-2017*, China Construction Industry Press, Beijing, China, 2017.